



# Preparation and characterization of UV-cured epoxy acrylate-based nanocomposite coatings containing organonanoclay

Murad Turna<sup>1</sup> · Ferhat Şen<sup>2</sup> · Seyfullah Madakbaş<sup>1</sup> · Sevim Karataş<sup>1</sup>

Received: 11 April 2022 / Revised: 21 June 2022 / Accepted: 15 July 2022 /  
Published online: 20 August 2022

© The Author(s), under exclusive licence to Springer-Verlag GmbH Germany, part of Springer Nature 2022

## Abstract

In this study, it is aimed to obtain UV-cured nanocomposite coatings. UV-curable epoxy acrylate resins were synthesized by reacting aliphatic-based epoxy resin with adipic acid and acrylic acid at certain rates and their chemical structures were characterized. The synthesized resins were reinforced with organonanoclay at different rates, applied as a film to plexiglass surfaces and cured with UV rays. The thermal properties, flammability, thermomechanical properties, surface properties, morphological properties, light transmittance and durability properties of the obtained nanocomposite coatings containing organonanoclay were investigated. With 5% organonanoclay reinforcement to the epoxy acrylate resin, the temperature of final mass loss increased from 521 to 557 °C, char yield increased from 0.02% to 2.95%, LOI increased from 22.1 to 23.5%, contact angle increased from 56 to 74°. The results showed that UV-cured nanocomposite coatings have the properties required by the coating industry, and these properties are improved with the addition of organonanoclay.

**Keywords** Nanocomposite · Coating · UV-cured · Epoxy acrylate · Organonanoclay

## Introduction

Coatings are used in many applications in our daily life, such as architectural wall coverings and automotive paints [1]. The use of coatings has two main purposes: decorative appearance and protective barrier. The main function of a coating is to protect the structure from major damages such as corrosion, scratches, peeling while

---

✉ Sevim Karataş  
skaratas@marmara.edu.tr

<sup>1</sup> Department of Chemistry, Marmara University, 34722 Istanbul, Türkiye

<sup>2</sup> Department of Food Processing, Zonguldak Bülent Ecevit University, 67900 Zonguldak, Türkiye

providing the desired appearance [2]. Furniture coatings protect against red wine, coffee or chemical spills that can damage furniture or its fabric, while automotive coatings protect against acid rain, tree resins and bird debris. Although most of the coatings are water-based, the coatings used in industry, vehicles, furniture, metal boxes, cardboards are organic solvent-based [3].

UV (Ultraviolet)-cured systems are mainly used in transparent coating applications. Therefore, high demands are placed on the performance of these systems [4]. It is important that it provides protection against many effects such as scratches on the coating surface, surface damage caused by chemicals, acid rain and bird droppings caused by air pollution. The formulations used for UV-cured coatings for this purpose depend on the specific performance requirements and the application technique. The basic compositions of UV-cured coatings are UV-curable resin, photoinitiator, and reactive diluent. The coating also contains stabilizers, pigments and fillers [5]. Cured of coatings is generally done by radical polymerization, but also by cationic mechanism [6].

UV-cured coatings have many advantages such as energy-saving, high production speed, solvent-free formulations, easy recycling, low surface temperature, high product durability, versatility, high scratch resistance, chemical resistance, resistance to abrasion, stain and solvent resistance [7]. On the other hand, there are drawbacks such as the high cost of the chemical materials used, hardening in the presence of UV stabilizers, oxygen inhibition on the surface, moisture sensitivity, difficulties experienced in pigmented coatings [8].

Polymer composite studies with functionalized nanoparticles have attracted a lot of attention in recent years [9]. Organonano-clays are an important reinforcing material used for this nanocomposite structures [10]. Organonano-clays are generally composed of montmorillonite clay structures. They are structures that contain aluminum or magnesium hydroxide in a double-layered silica structure. Therefore, they can easily penetrate between water and other polar molecules [11]. In recent years, a lot of work has been done on organonano-clays. For example, Rao et al. prepared carbon phenolic composites containing organo-modified montmorillonite nanoclay in different ratios and investigated the mechanical, thermal and ablation properties of the obtained materials. According to the results obtained, it has been reported that the sample containing 2% nanoclay provides optimum thermal stability without compromising mechanical properties and ablative properties [12]. Zawawi et al. prepared nanocomposites by adding 1, 3, 5 and 7% organonano-clay to the polylactic acid and polypropylene mixture. The thermal, mechanical and morphological properties of the obtained nanocomposites were investigated. According to the results obtained, it has been reported that the amount of the performing supplement is in the range of 1–3% [13]. Pumchusak et al. developed phenolic composites containing 0.5–2.5% organo-modified montmorillonite nanoclay and investigated the mechanical, thermo-mechanical and thermal properties of the developed composites. They reported that the product with optimum properties was the product containing 1.5% reinforcement material [14].

In this study, UV-curable nanocomposite materials containing organonano-clay with superior properties required by the coating industry were developed. For this purpose, three different epoxy acrylate resins were synthesized and UV cured

nanocomposite coatings were obtained by adding organonano clay at different rates to these resins. The structural characterization of the resins and the thermal properties, flammability, thermomechanical properties, surface properties, morphological properties, light transmittance and durability of the obtained materials were investigated.

## Experimental

### Materials

Trimethylolpropane triglycidyl ether (epoxy, Heloxy Modifier TP, epoxy content: 30%) was purchased from Hexion. Triphenylphosphine (TPP), adipic acid, hydroquinone, acrylic acid, *N*-vinyl pyrrolidone (NVP), trimethylolpropane acrylate (TMPTA), 2-hydroxy-2-methylpropiophenone, acetone, hydrochloric acid, sulfuric acid, acetic acid, xylene and methanol were purchased from Sigma Aldrich. Organonano clay was purchased from Nanocor. Its average dry particle size is 18–23 nm. All chemicals were supplied in high purity and used directly without purification.

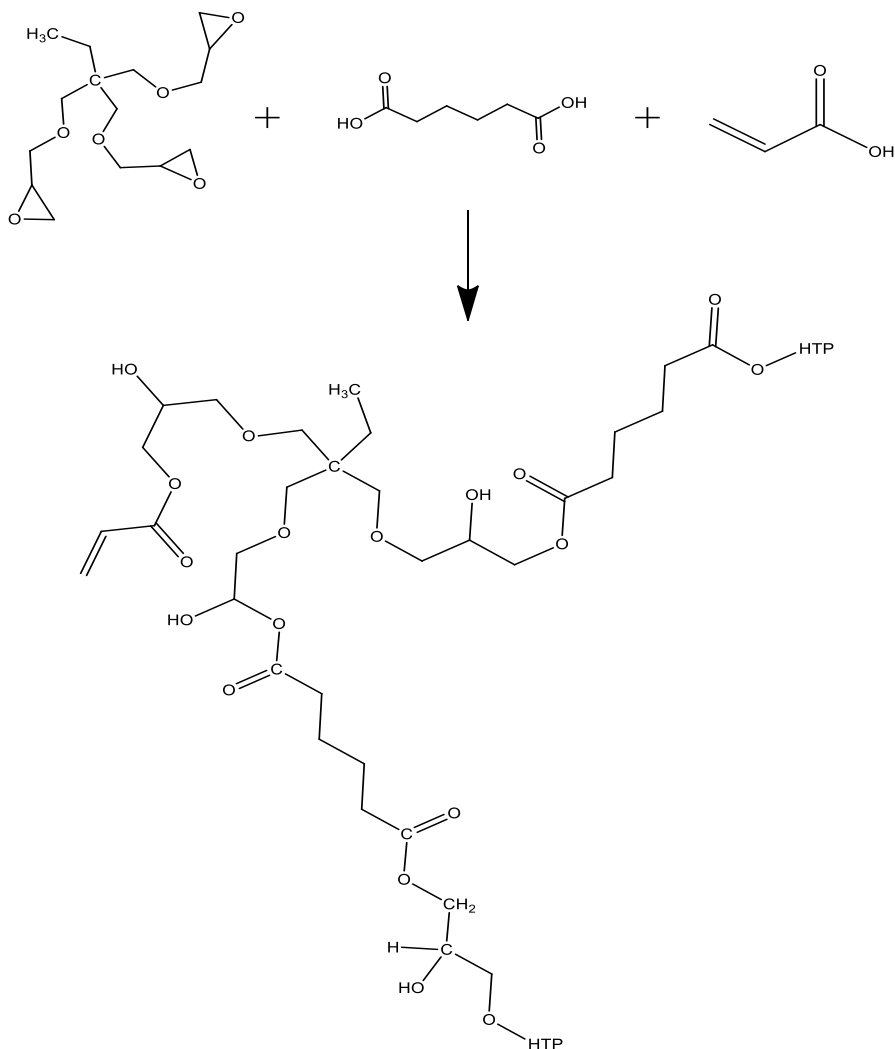
### Synthesis of epoxy acrylate resins

The content of epoxy acrylate resins was calculated according to the epoxy content (30%) of Heloxy Modifier TP and shown in Table 1. Heloxy Modifier TP and TPP were added to a reaction flask and the system temperature was gradually increased to 85 °C. Adipic acid was added slowly and the reaction was stirred for 2 h. At the end of the period, the temperature was reduced to 45 °C and hydroquinone was added to prevent polymerization that may occur in the environment. Acrylic acid was added dropwise to the mixture. The temperature was gradually increased to 80 °C and the reaction was stirred for 4 h. At the end of the period, the temperature was reduced to 30 °C and epoxy acrylate resin was obtained. The contents of epoxy acrylate resins are shown in Table 1 and the reaction scheme is shown in Scheme 1.

<sup>1</sup>H NMR of EA (CD<sub>3</sub>COCD<sub>3</sub>, ppm): 6.43–6.35 (-CH<sub>i</sub> H<sub>j</sub>=CH-), 6.23–6.12 (-CH<sub>i</sub> H<sub>j</sub>=CH<sub>h</sub>-), 5.95–5.85 (-CH<sub>i</sub> H<sub>j</sub>=CH-), 4.28–4.20 (-CH<sub>2</sub>-O-CO-HC=), 4.05–4.00 (-CH-OH-), 3.51–3.45 (-O-CH<sub>2</sub>-CH-OH), 3.41–3.32 (-O-CH<sub>2</sub>-C-), 3.13–3.03 (-CH-OH), 2.07 (CD<sub>3</sub>COCD<sub>3</sub>), 1.50–1.30 (-CH<sub>2</sub>-CH<sub>3</sub>), 0.96–0.77 (-CH<sub>2</sub>-CH<sub>3</sub>).

**Table 1** Contents of epoxy acrylate resins

Resins	Heloksy modifier TP (mol)	Adipic acid (mol)	Acrylic acid (mol)	Triphenylphosphine (mol)	Hydroquinone (mol)
EA	0.1395	–	0.1325	0.1143	0.0003
EA-AA:15	0.1395	0.0209	0.1186	0.1143	0.0003
EA-AA:30	0.1395	0.0419	0.0977	0.1143	0.0003



**Scheme 1** Synthesis of epoxy acrylate resins

$^1\text{H}$  NMR of EA-AA:30 ( $\text{CD}_3\text{COCD}_3$ , ppm): 6.43–6.32 ( $-\text{CH}_i$   $\text{H}_j = \text{CH}-$ ), 6.23–6.04 ( $-\text{CH}_i$   $\text{H}_j = \text{CH}_i-$ ), 5.97–5.78 ( $-\text{CH}_i$   $\text{H}_j = \text{CH}-$ ), 4.21–4.10 ( $-\text{CH}_2-\text{O}-\text{CO}-\text{CH}=\text{}$ ), 4.02–3.92 ( $-\text{CH}-\text{OH}-$ ), 3.60–3.53 ( $-\text{O}-\text{CH}_2-\text{CH}-\text{OH}$ ), 3.34–3.33 ( $-\text{O}-\text{CH}_2-\text{C}-$ ), 3.13–3.02 ( $-\text{CH}-\text{OH}$ ), 2.42–2.30 ( $-\text{O}-\text{CO}-\text{CH}_2-$ , adipic acid), 2.07 ( $\text{CD}_3\text{COCD}_3$ ), 1.74–1.60 ( $-\text{CH}_2-\text{CH}_2-$ , adipic acid), 1.47–1.32 ( $-\text{CH}_2-\text{CH}_3$ ), 0.95–0.80 ( $-\text{CH}_2-\text{CH}_3$ ).

FT-IR of epoxy acrylate resins ( $\text{cm}^{-1}$ ): 3440 ( $-\text{OH}$ ), 2880 ( $-\text{CH}$ ), 1720 (carbonyl), 1630 ( $\text{C}=\text{C}$ ), 1270 ( $-\text{C}-\text{O}$ ), 1093 ( $\text{C}-\text{O}-\text{C}$ ), 809 (acrylate).

## Preparation of UV-cured coatings

Coating formulations mixtures were prepared by adding NVP as a diluent reagent, TMPTA as a crosslinker, and 2-hydroxy-2-methylpropiophenone as a photoinitiator, organonano clay as a reinforcing agent, to the synthesized epoxy acrylate resins at the rates shown in Table 2. All formulations were kept in an ultrasonic bath at 50 °C for 2 h to mix homogeneously. Homogeneous formulations were poured into a Teflon mold, they were kept under a UV lamp (Osram Ultrawit 300 model 300 Watt) for 3 min and UV-cured coatings were obtained with the dimensions of 50 × 10 × 1 mm. An illustration showing the preparation of UV-cured coatings is shown in Scheme 2.

## Measurements and characterization

Perkin Elmer Spectrum 100 branded FT-IR device was used for the structural characterization of epoxy acrylate resins. In addition, Omnicure UV lamp device and real-time FT-IR were used to determine the double bond conversion percentages of UV curable formulations.

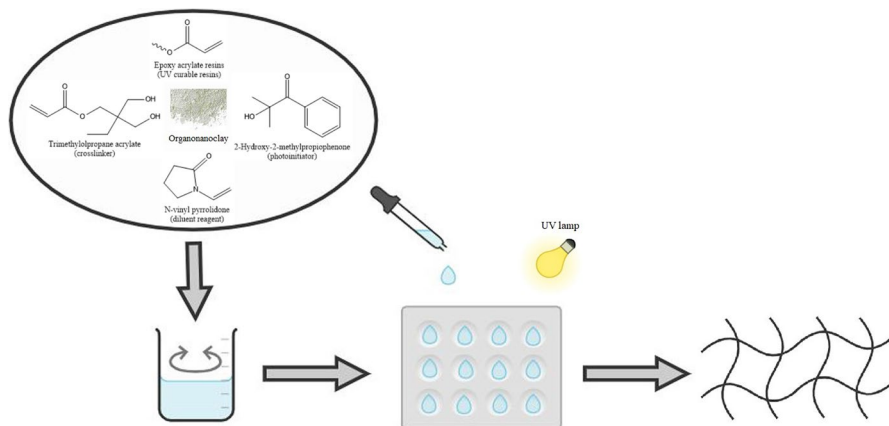
The Varian Mercury-VX 400 MsHz BB brand NMR device was used to determine the molecular structure of epoxy acrylate resins.

XRD analysis was performed to examine the distribution of organonano clay used in UV curing coatings. Measurements were made with PANalytical brand X'Pert PRO model XRD device in the range of 2–60 degrees.

Perkin Elmer thermogravimetric analysis (TGA) device was used to determine the thermo-oxidative stability of UV-cured coatings. The samples were heated from 30 to 800 °C under an air atmosphere at a rate of 10 °C/min.

**Table 2** Contents of UV-cured coatings

Samples	Resin (%)	NVP (%)	TMPTA (%)	Photoinitiator (%)	Organonano-clay (%)
EA	77	10	10	3	–
EA/1	77	10	10	3	1
EA/3	77	10	10	3	3
EA/5	77	10	10	3	5
EA-AA:15	77	10	10	3	–
EA-AA:15/1	77	10	10	3	1
EA-AA:15/3	77	10	10	3	3
EA-AA:15/5	77	10	10	3	5
EA-AA:30	77	10	10	3	–
EA-AA:30/1	77	10	10	3	1
EA-AA:30/3	77	10	10	3	3
EA-AA:30/5	77	10	10	3	5



**Scheme 2** Preparation of UV-cured coatings

The minimum oxygen amount required for the samples fixed in a glass jar with nitrogen and oxygen concentrations to burn for a maximum of 180 s was determined as the Limiting Oxygen Index (LOI) of the UV curing coatings.

Thermomechanical properties of UV-cured coatings were determined by dynamic mechanical analysis (DMA) performed on a PerkinElmer DMA 8000 analyzer in the tension mode. Tension was applied to the samples at a frequency of 1 Hz and with a heating of 4 °C/min between 30 and 200 °C.

In order to determine the hydrophobic properties of UV-cured coatings, the contact angles of the samples with the pure water drop were measured using the Krüss DSA 10 device. Five measurements were taken for each sample and the average of the results was used.

The light transmittance of UV-cured coatings was determined using Shimadzu brand UV-2450 model UV–visible spectrophotometer.

The soxhlet extraction method was used to determine the gel amount of UV-cured coatings. The first weighing of the samples was taken, extracted with acetone for 12 h and dried in a vacuum oven at 50 °C for one hour. The dried samples were weighed again. The gel amount of the samples was determined by proportioning the last and the first weighing.

Swelling test was performed to measure the water-resistance of UV-cured coatings. In this test, the samples were weighed and kept in distilled water for 24 h. The surfaces of the samples removed from the water were dried and weighed again. The swelling amount of the samples was determined by proportioning the amount of water absorbed by the sample to the initial weighing. With the same method, the samples were kept in 10% hydrochloric acid solution, 10% sulfuric acid solution, 10% acetic acid solution, xylene, methanol, and their chemical resistance was determined.

Adhesion degrees of the samples were determined using the Gardco Paint Adhesion Test Kit.

The morphology of UV-cured coatings was analyzed with a Philips XL30 ESEM-FEG device. The samples were fractured with the help of liquid nitrogen before examination and the fractured surfaces were covered with platinum.

## Results and discussion

### FT-IR Spectroscopy of epoxy acrylate resins

FT-IR spectra of Heloxy Modifier TP and obtained epoxy acrylate resins are shown in Fig. 1. It was originated that the band at  $1093\text{ cm}^{-1}$  is from the C–O–C group, the band at  $3440\text{ cm}^{-1}$  is from the –OH group, the band at  $2880\text{ cm}^{-1}$  is from –CH bonds, the band at  $1630\text{ cm}^{-1}$  is from the C=C bonds, the band at  $1270\text{ cm}^{-1}$  is from the –C–O group. the band at  $809\text{ cm}^{-1}$  is from acrylate groups. The formation of a carbonyl band around  $1720\text{ cm}^{-1}$  in the FT-IR spectra of epoxy acrylate resins and the disappearance of the epoxy band observed around  $900\text{ cm}^{-1}$  show that desired reaction has been successfully achieved by opening the epoxy rings [15–17].

### $^1\text{H}$ NMR Spectroscopy of epoxy acrylate resins

$^1\text{H}$  NMR spectrum of EA is shown in Fig. 2a,  $^1\text{H}$  NMR spectrum of EA-AA:30 is shown in Fig. 2b. Observation of peak of proton in the –OH group in the range of 3.03–3.13 ppm in Fig. 2a confirms the opening of the epoxy ring. In addition, observation of peaks belonging to protons in the acrylic acid group in the range of

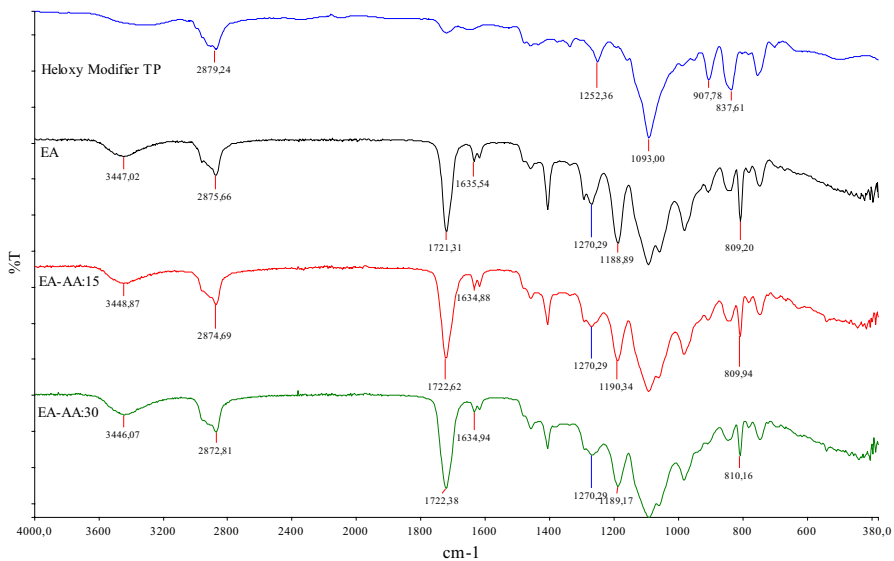
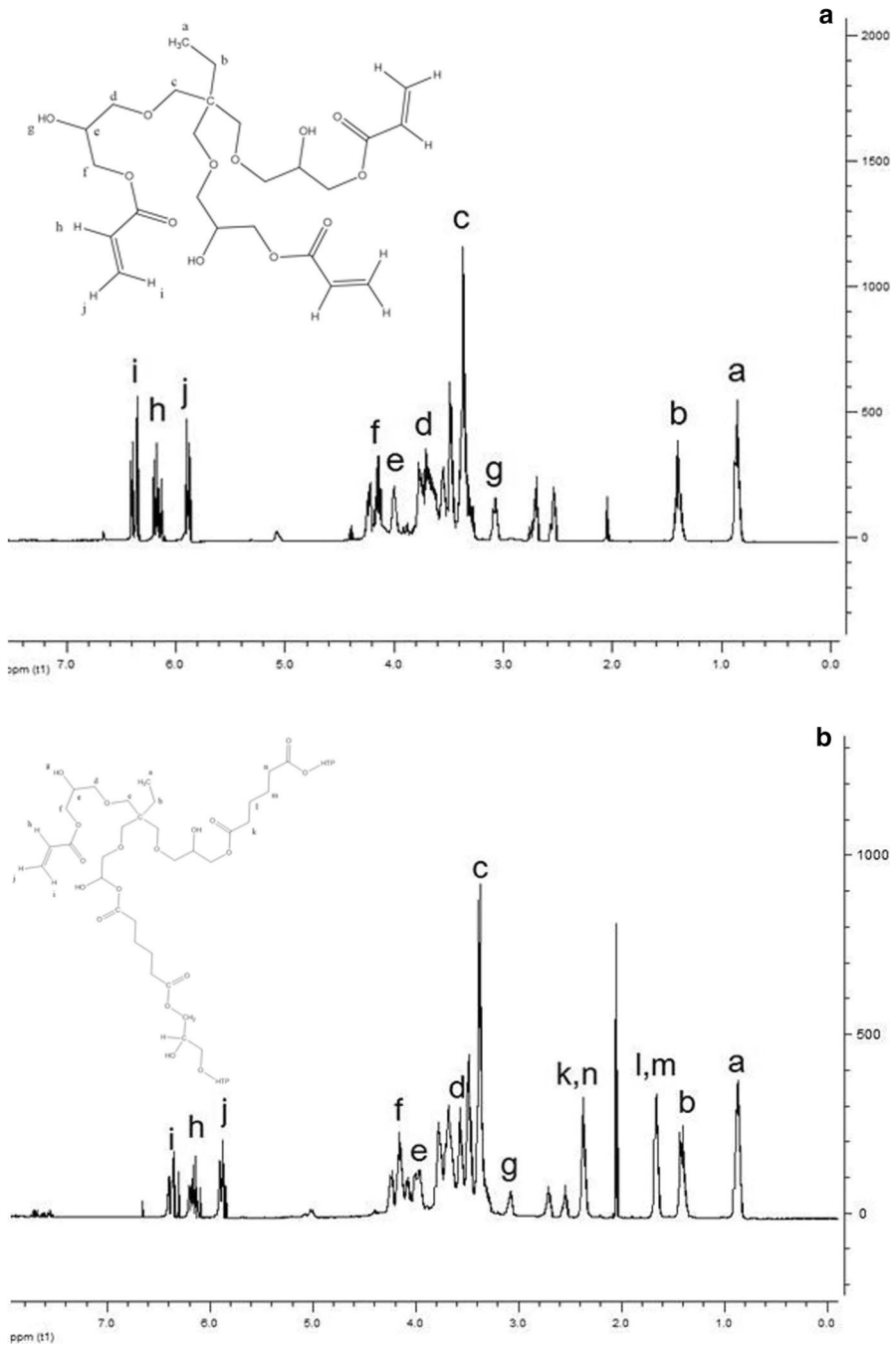


Fig. 1 FT-IR spectra of heloxy modifier TP and epoxy acrylate resins



**Fig. 2**  $^1\text{H}$  NMR spectra of epoxy acrylate resins, **a** EA and **b** EA-AA:30

5.85–6.43 proves that acrylic acid binds successfully to Heloxy Modifier TP. On the other hand, when Fig. 2b is examined, observation of peak belonging to proton in the -OH group in the range of 3.02–3.13 ppm confirms the opening of the epoxy ring. Moreover, observation of peaks of acrylic acid protons in the range of 5.78–6.43 ppm, and the peaks of adipic acid protons in the range of 1.60–1.74 ppm and 2.30–2.42 ppm proves that both acrylic acid and adipic acid bind successfully to Heloxy Modifier TP. As a result, it was determined that all the peaks were in harmony with the chemical structure of the synthesized resins [18, 19].  $^1\text{H}$  NMR results support the successful synthesis of the resins.

### UV-curing reaction kinetics

UV-curing reaction kinetics were investigated through the conversion of C=C acrylate double bond peaks at  $810\text{ cm}^{-1}$  and  $1634\text{ cm}^{-1}$  in real-time FT-IR. For this, the resins on the prepared KBr tablets were interacted with UV for 3 min and the real-time FT-IR spectra were recorded in the range of  $400\text{--}4000\text{ cm}^{-1}$ . Acrylate peak transformations between the first and last seconds were examined and double bond conversions were calculated as percentages. Double bond transformations at  $810\text{ cm}^{-1}$  are shown in Fig. 3, and double bond transformations at  $1634\text{ cm}^{-1}$  are shown in Fig. 4. It has been determined that double bond conversions occur in a very short time and double bond conversion rates are between 80 and 100%. These results proved that UV-curing is fast and highly successful.

### XRD analysis of UV-cured coatings

XRD measurements were performed between  $2\theta=2\text{--}60$  at 45 kV and 40 mA with a  $\text{CuK}_\alpha$  radiation ( $n=1.54\text{ \AA}$ ) brand diffractometer. The resulting patterns are shown in Fig. 5. When the XRD graph of the organonano clay is examined, it is seen that the polymer chains intercalate within the silicate layers between  $2\theta=2.7\text{--}16$  degrees [20]. The characteristic peak of organonano clay is observed at  $2\theta=4.11$ . This characteristic peak of organonano clay is observed at low angles ( $d\text{ spacig}=2.174404\text{ nm}$ ) in all composites. Due to the reduction of coherent layer scattering, the peak intensity of composite/organonano clay decreases. This shows the intercalation between polymer chains and clay layers. When the XRD graphs are examined, it is seen that the crystal structure deteriorates and turns into an amorphous structure with doping. When the graphs of organonano clay and composite-organonano clay are compared, it can be interpreted that the crystal structure turns into an amorphous structure, in which 10 peaks seen in organonano clay turn into a prominent peak at  $2\theta=2.7$  and a weak indistinct peak at  $2\theta=16$  seen in the composite-organonano clay structure.

### Thermal stability and flammability of UV-cured coatings

The thermal properties of the obtained resins and UV-cured coatings were investigated by TGA. TGA thermograms are shown in Fig. 6 and the results obtained

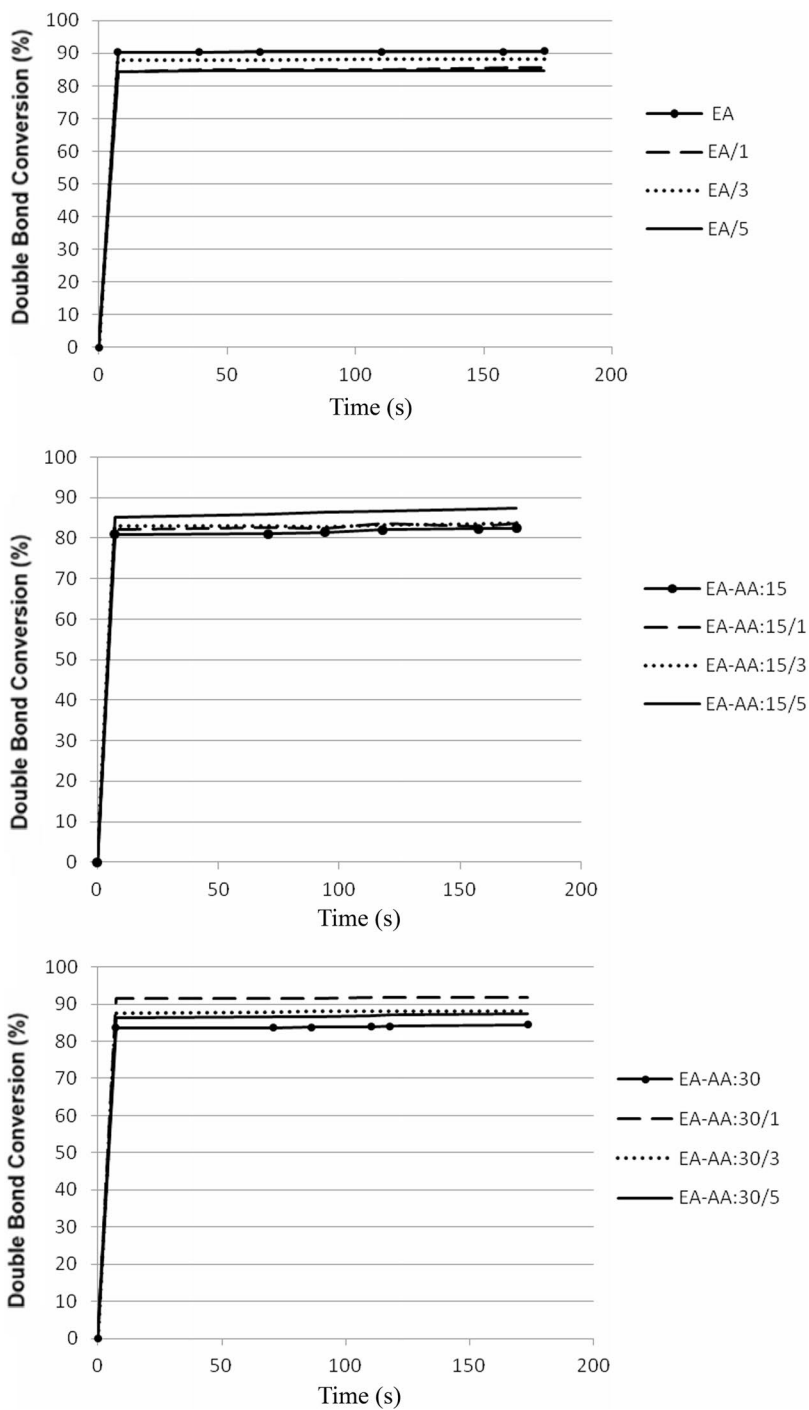


Fig. 3 Conversion of C=C acrylate double bond peaks at  $810\text{ cm}^{-1}$

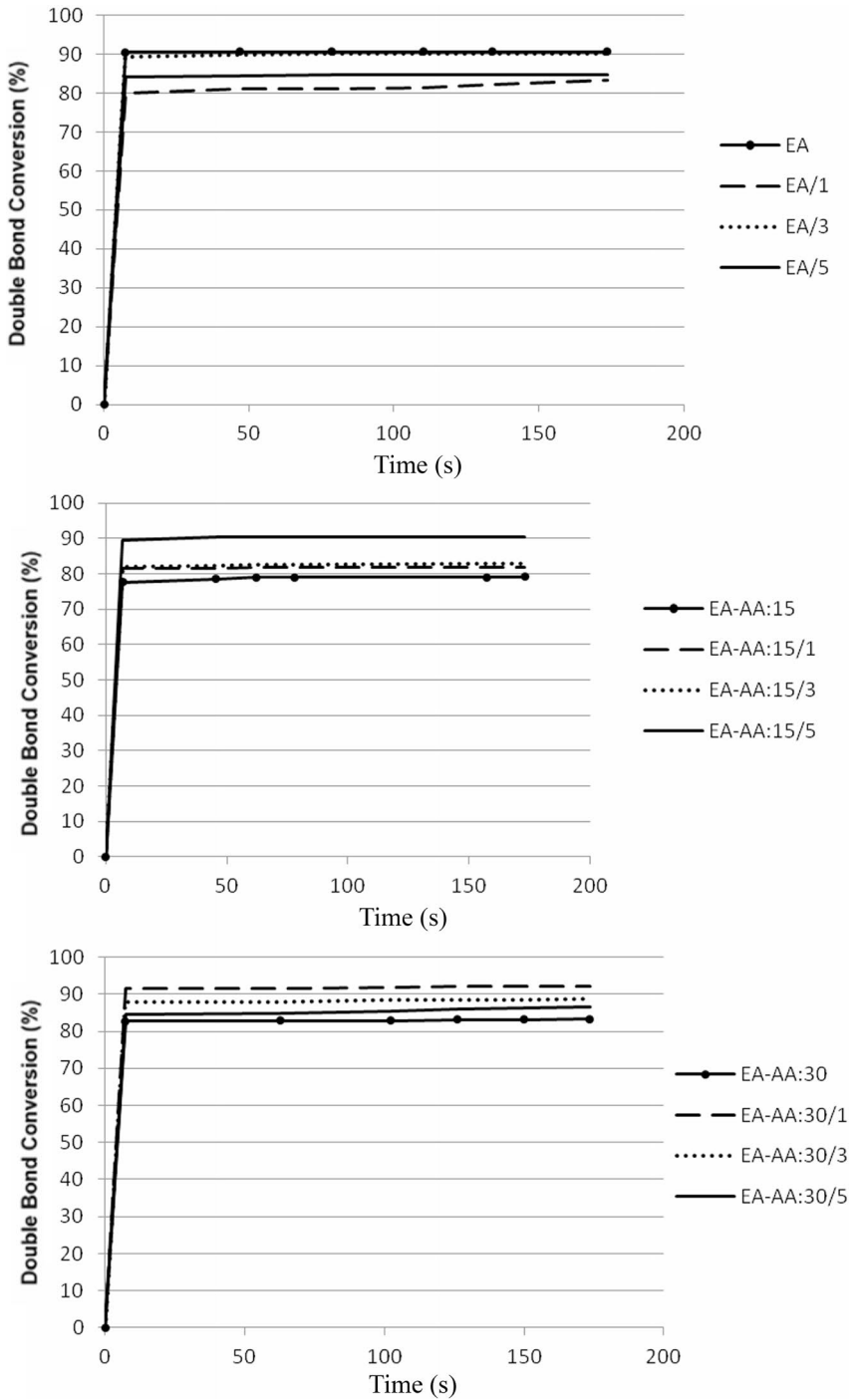
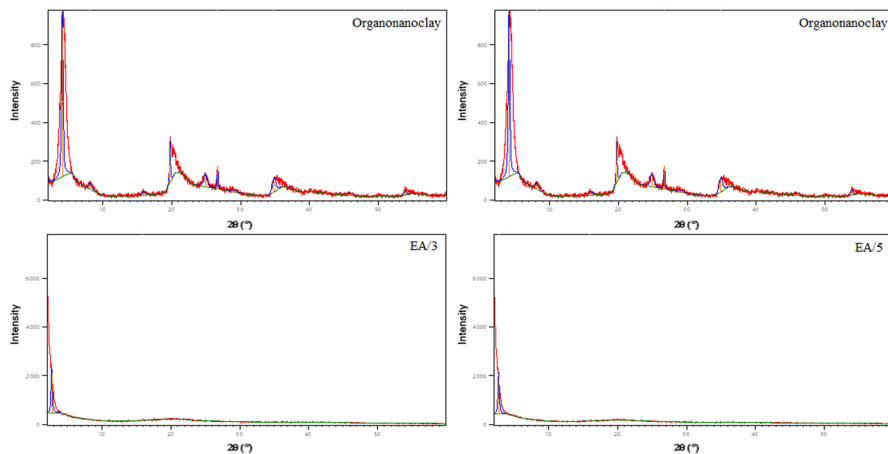


Fig. 4 Conversion of C=C acrylate double bond peaks at  $1634\text{ cm}^{-1}$



**Fig. 5** XRD patterns of UV-cured coatings

from them in Table 3. While the initial mass loss of EA resin is at 327 °C, the initial mass losses of EA-AA:15 and EA-AA:30 are 335 and 341 °C, respectively. These results showed that 15% and 30% adipic acid additions improved the thermal properties of EA resin. It was determined that the thermal properties of the materials obtained when 1%, 3% and 5% organonano clay were added to EA, EA-AA:15 and EA-AA:30 resins were better than the thermal properties of the resins. In addition, when the char yield of the coating materials was examined, the char yield of EA was 0.022%, while the char yield of EA/1, EA/3 and EA/5 were determined as 2.951%, 3.695% and 3.445%, respectively. While the char yield of EA-AA:15 is 0.013%, the char yield of EA-AA:15/1, EA-AA:15/3 and EA-AA:15/5 is 1.221%, 2.428% and 3.695%, respectively. While the char yield of EA-AA:30 was 0.045%, the char yield of EA-AA:30/1, EA-AA:30/3 and EA-AA:30/5 was found to be 1.090%, 2.190% and 3.445%, respectively. These results showed that as organonano clay was added to the resins, the char yield increased, so the fire resistance of the material increased [21].

The LOI test was performed to measure the minimum oxygen concentration required for the UV-cured coatings to ignite. According to the LOI results in Table 3., it is seen that the inflammability of the material increased with the addition of organonano clay. As can be seen from the results, the additions of adipic acid and organonano clay to the epoxy acrylate resin increase the LOI amounts. The results obtained are compatible with the literature. For example, El-Fattah et al. prepared polyurethane nanocomposites containing organo-modified nano clay and reported that LOI values increased as the amount of organo-modified nano clay increased [22].

### Thermomechanical properties of UV-cured coatings

Thermomechanical properties of UV-cured coatings were determined by DMA. DMA curves of the samples are shown in Fig. 7, and the storage modules ( $E'$ ) at

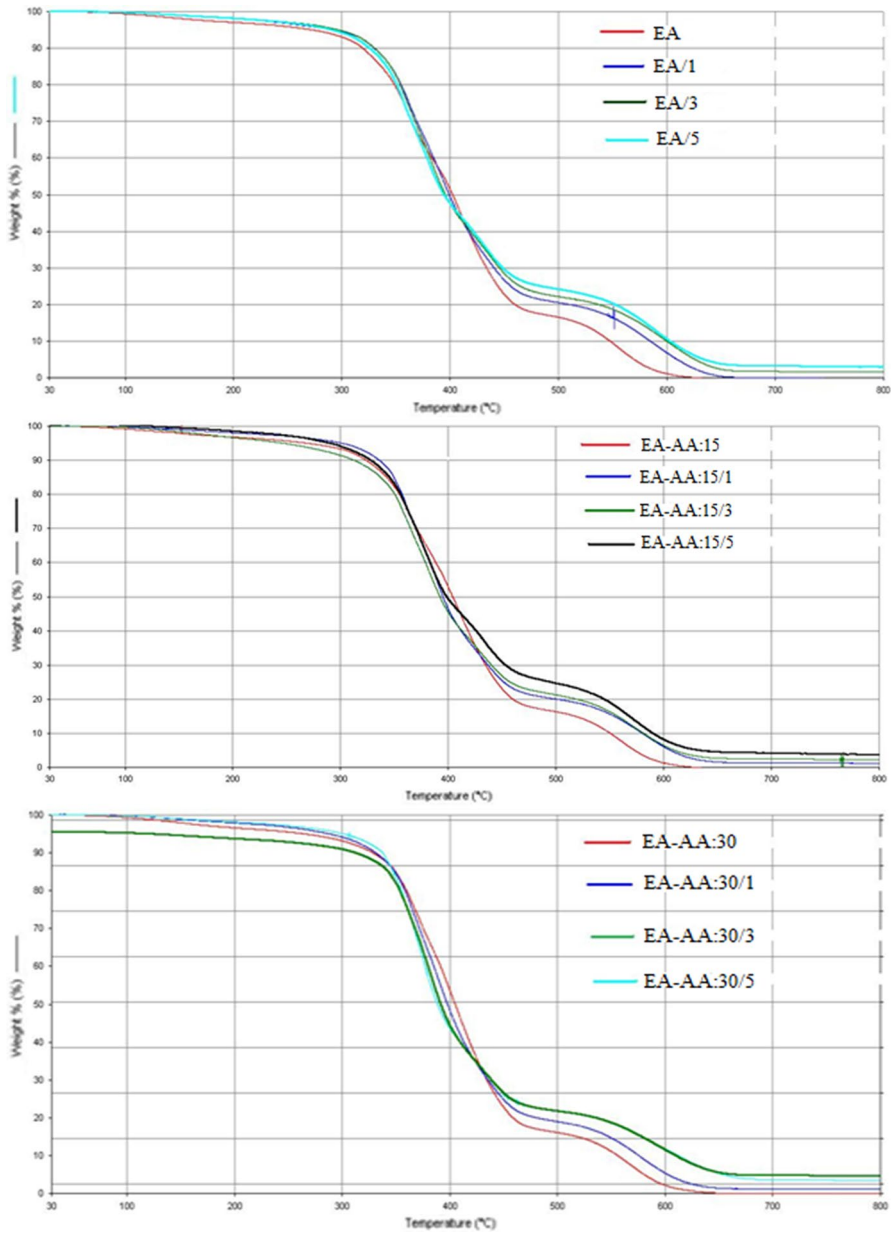


**Fig. 6** Thermograms of UV-cured coatings

50 °C are shown in Table 3. When the results are examined, it is seen that the storage modulus generally decreases as the adipic acid ratio increases and the acrylic acid ratio decreases in the formulations. For example, while the storage modulus of EA was 1232 MPa, 868 MPa for EA-AA:15 and 440 MPa for EA-AA:30 were

**Table 3** Thermal stability, flammability, thermomechanical properties and gel amount of UV-cured coatings

Samples	5% Mass loss (°C)	Initial mass loss (°C)	Final mass loss (°C)	Char yield (%)	LOI (%)	$E'$ at 50 °C (MPa)	Gel amount (%)
EA	280	327	521	0.022	22.1	1232	98.9
EA/1	284	336	458	0.042	22.5	478	97.7
EA/3	297	336	547	1.485	23.0	829	98.6
EA/5	294	333	557	2.957	23.5	1089	97.0
EA-AA:15	276	335	441	0.013	22.5	868	97.3
EA-AA:15/1	309	341	531	1.221	23.8	1139	98.1
EA-AA:15/3	242	333	529	2.428	24.5	616	94.6
EA-AA:15/5	294	338	536	3.695	25.3	2578	98.1
EA-AA:30	271	341	520	0.045	23.1	440	98.5
EA-AA:30/1	295	336	530	1.090	24.2	773	98.2
EA-AA:30/3	303	342	538	2.190	24.5	490	98.6
EA-AA:30/5	305	342	554	3.445	25.1	513	98.4

found at 50 °C. This decrease is attributed to the decrease in crosslink density and the formation of a more flexible structure with the increase in the ratio of adipic acid containing more alkyl groups in formulations. It is not possible to see the regular decreasing trend in the storage modulus of the samples containing organonano clay. Because organonano clay nanoreinforcement allows the formation of organic–inorganic hybrid nanocomposite structures by changing the behavior of crosslinks.

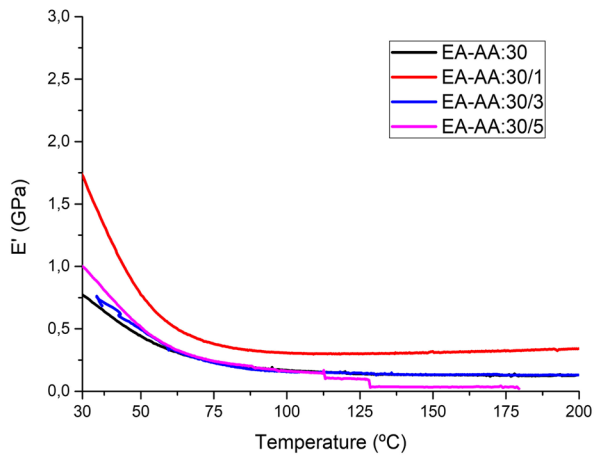
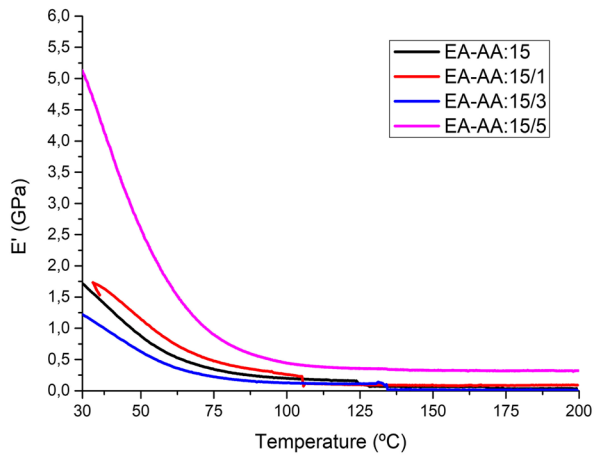
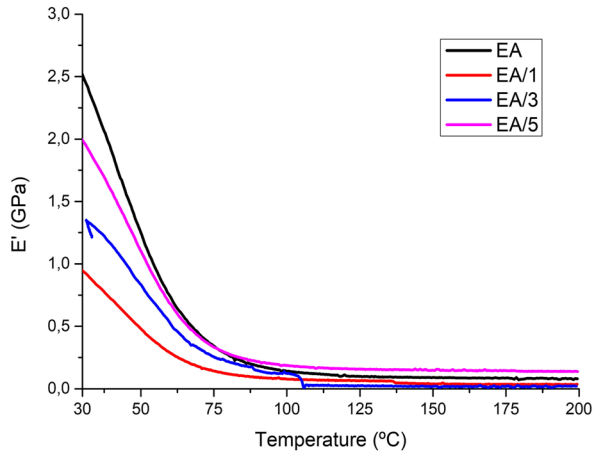
### Surface properties of UV-cured coatings

Contact angle measurement was performed to examine the hydrophobic properties of UV-cured coatings. The contact angle values and photographs obtained after dropping deionized water on the coated surfaces are shown in Fig. 8. While the contact angle of the EA sample is 56, the contact angle values of the EA-AA:15 and EA-AA:30 samples are 44 and 47, respectively. This shows that adipic acid makes the surface of the coating material hydrophilic. On the other hand, it is seen that there is an increase in the contact angles of the materials as the amount of organonano clay increases in the formulations.

### Light transmittance of UV-cured coatings

The light transmittance of the obtained materials was examined by spectrophotometer. The UV–visible diagrams of the samples are shown in Fig. 9. When the results are examined, there is no significant change in the light transmittance in the visible region as adipic acid is added to the samples. However, it is seen that the light transmittance in the visible region decreases as the organonano clay is added to each of

**Fig. 7** DMA curves of UV-cured coatings



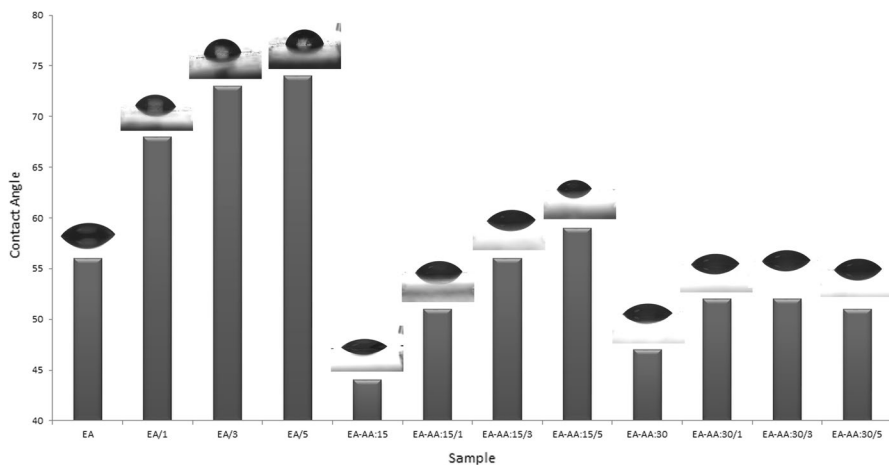


**Fig. 8** Contact angles of UV-cured coatings

the EA, EA-AA:15 and EA-AA:30 resins. These results show that adipic acid added to the resin does not affect the transparency of the coating material, but the addition of organonano clay reduces the transparency. Mallakpour et al. prepared polyvinyl-alcohol/organonano clay bionanocomposites and reported that the light transmittance decreased as the amount of organonano clay increased [23]. This shows that the obtained results are in agreement with the literature.

### Durability properties of UV-cured coatings

In order to determine the cross-link density of the samples, the materials were extracted using acetone for 3 h with the soxhlet extraction method. The samples, which remained undissolved in acetone as a result of the extraction, were dried in a vacuum oven at 45 °C for 24 h, their weights were taken and their gel amounts were calculated as percent. The results obtained are shown in Table 3. The gel amount of all samples was determined to be between 94–99%. These results show that the gel ratio in the coating material is quite high.

Swelling test was carried out to measure the resistance of the samples against water. After the samples were weighed, they were kept in distilled water for 24 h. The samples, whose surfaces were dried in a vacuum oven, were weighed again and their swelling amount was calculated as percent. The results obtained show that the swelling of all samples is less than 1%. These results prove that the water-resistance of the coating materials is quite good.

After the samples were weighed to measure their resistance to various chemical substances (acid, solvent, etc.), they were kept in 10% hydrochloric acid, 10% sulfuric acid, 10% acetic acid and methanol, xylene for 24 h. The samples were dried in a vacuum oven and weighed again. All samples were found to have less than 1% mass loss for all chemicals. These results show that all samples are highly resistant to chemicals.

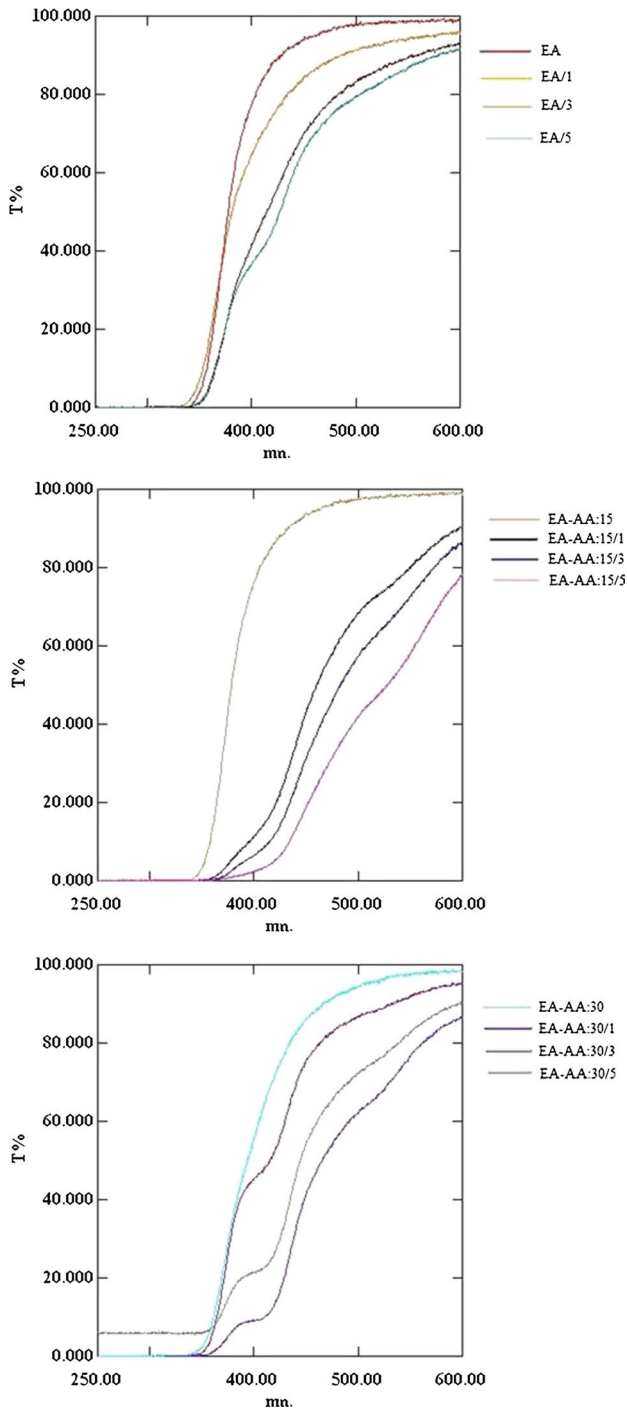


Fig. 9 UV-visible diagrams of UV-cured coatings

In order to ensure better adhesion of all formulations to the plexiglass surfaces, the plexiglasses were corona treated, then coated with the formulations and cured with UV. Adhesion of the coated surfaces was made by cross-cut-adhesion test, which was tested by drawing #. The adhesion degree of all samples was found to be 0. According to these results, it was determined that the formulations adhered very well to the plexiglass surfaces.

### Morphologies of UV-cured coatings

The surface morphology of UV-cured coatings was examined by scanning electron microscopy (SEM). The samples were first broken in liquid nitrogen, then the broken surfaces were covered with platinum and examined in the SEM device. SEM images with  $\times 10,000$  resolution obtained as a result of the examination are shown in Fig. 10. It was observed that all samples had a homogeneous structure and the components in the formulations were in harmony with each other. In addition, the particle sizes are between 120–135 nm in the EA/3 sample, between 47–80 nm in the EA/5 sample, between 94–231 nm in the EA-AA:30 sample, and between 73–133 nm in the EA-AA:30/3 sample. It was measured between 84–120 nm in the EA-AA:30/5 sample.

### Conclusions

In this study, three different epoxy acrylate resins were synthesized and UV cured nanocomposite coatings were obtained by adding organonano clay at different rates to these resins. FT-IR and  $^1\text{H-NMR}$  spectroscopies showed successful synthesis of the resins. From the studies on XRD and UV curing reaction kinetics, it was understood that the coatings were obtained with a  $\text{C}=\text{C}$  double bond conversion ratio of more than 80%. In nanocomposite coating formulations, it was observed that the char yield, LOI, contact angles increased, and the light transmittance decreased as the amount of organonano clay increased. It was determined that the storage modulus decreased with the increase in the adipic acid ratio and the decrease in the acrylic acid ratio in the formulations. It was determined that the gel content of the coatings was quite high, highly resistant to water and chemicals, and had good adhesion properties. In addition, according to the SEM analysis results, it was observed that the samples were in a homogeneous structure and the components in the formulations were in harmony with each other. When all the results are evaluated, it is seen that the obtained UV-cured nanocomposite coatings have the properties required by the coating industry, and these properties were improved with the addition of organonano clay.

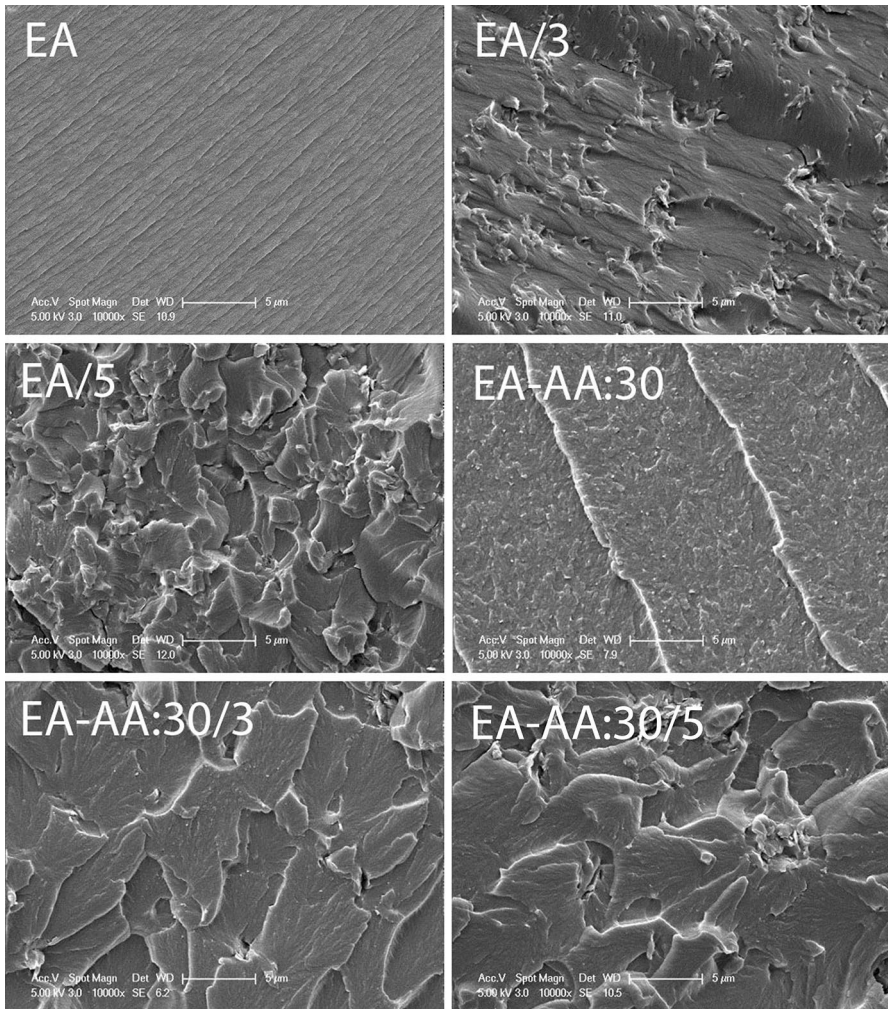


**Fig. 10** SEM images of UV-cured coatings

**Acknowledgements** This work was supported by Marmara University, Commission of Scientific Research Project under the project FEN-C-YLP-250416-0191.

## References

1. Bai Y, Zhang H, Shao Y, Zhang H, Zhu J (2021) Recent progresses of superhydrophobic coatings in different application fields: an overview. *Coatings* 11:116. <https://doi.org/10.3390/coatings11020116>
2. Wagle PG, Tamboli SS, More AP (2021) Peelable coatings: a review. *Prog Org Coat* 150:106005. <https://doi.org/10.1016/j.porgcoat.2020.106005>
3. Jiao C, Sun L, Shao Q, Song J, Hu Q, Naik N, Guo Z (2021) Advances in waterborne acrylic resins: synthesis principle, modification strategies, and their applications. *ACS Omega* 6:2443–2449. <https://doi.org/10.1021/acsomega.0c05593>

4. Jiao X, Liu J, Jin J, Cheng F, Fan Y, Zhang L, Lai G, Hua X, Yang X (2021) UV-cured transparent silicone materials with high tensile strength prepared from hyperbranched silicon-containing polymers and polyurethane-acrylates. *ACS Omega* 6:2890–2898. <https://doi.org/10.1021/acsomega.0c05243>
5. Liu F, Liu A, Tao W, Yang Y (2020) Preparation of UV curable organic/inorganic hybrid coatings-a review. *Prog Org Coat* 145:105685. <https://doi.org/10.1016/j.porgcoat.2020.105685>
6. Bednarczyk P, Mozelewska K, Nowak M, Czech Z (2021) Photocurable epoxy acrylate coatings preparation by dual cationic and radical photocrosslinking. *Materials* 14:4150. <https://doi.org/10.3390/ma14154150>
7. Hermann A, Giljean S, Pac MJ, Marsiquet C, Beauflis-Marquet M, Burr D, Landry V (2021) Understanding indentation, scratch and wear behavior of UV-cured wood finishing products. *Prog Org Coat* 161:106504. <https://doi.org/10.1016/j.porgcoat.2021.106504>
8. Czachor-Jadacka D, Pilch-Pitera B (2021) Progress in development of UV curable powder coatings. *Prog Org Coat* 158:106355. <https://doi.org/10.1016/j.porgcoat.2021.106355>
9. Pieliowski K, Majka TM (2019) Polymer composites with functionalized nanoparticles. Elsevier. <https://doi.org/10.1016/B978-0-12-814064-2.00011-1>
10. Suhas DP, Aminabhavi TM, Raghu AV (2014) para-Toluene sulfonic acid treated clay loaded sodium alginate membranes for enhanced pervaporative dehydration of isopropanol. *Appl Clay Sci* 101(2014):419–429. <https://doi.org/10.1016/j.clay.2014.08.017>
11. Beyki MH, Shemirani F, Khani R (2014) Green preconcentration of trace amounts of copper from water and food samples onto novel organo-nanoclay prior to flame atomic absorption spectrometry. *J AOAC Int* 97:1426–1433. <https://doi.org/10.5740/jaoacint.12-212>
12. Rao GR, Srikanth I, Reddy KL (2021) Effect of organo-modified montmorillonite nanoclay on mechanical, thermal and ablation behavior of carbon fiber/phenolic resin composites. *Def Technol* 17:812–820. <https://doi.org/10.1016/j.dt.2020.05.012>
13. Zawawi EZE, Noor Hafizah AH, Romli AZ, Yuliana NY, Bonnia NN (2021) Effect of nanoclay on mechanical and morphological properties of poly(lactide) acid (PLA) and polypropylene (PP) blends. *Mater Today Proc* 46:1778–1782. <https://doi.org/10.1016/j.matpr.2020.07.612>
14. Pumchusak J, Thajina N, Keawsujai W, Chaiwan P (2021) Effect of organo-modified montmorillonite nanoclay on mechanical, thermo-mechanical, and thermal properties of carbon fiber-reinforced phenolic composites. *Polymers* 13:754. <https://doi.org/10.3390/polym13050754>
15. Salih AM, Ahmad MB, Ibrahim NA, Dahlan KZHM, Tajau R, Mahmood MH, Yunus WMZW (2015) Synthesis of radiation curable palm oil-based epoxy acrylate: NMR and FTIR spectroscopic investigations. *Molecules* 20:14191–14211. <https://doi.org/10.3390/molecules200814191>
16. Zhang K, Li L, Chen X, Lu C, Ran J (2022) Controlled preparation and properties of acrylic acid epoxy-acrylate composite emulsion for self-crosslinking coatings. *Appl Polym Sci* 139:51441. <https://doi.org/10.1002/app.51441>
17. Reddy KR, Raghu AV, Jeong HM (2008) Synthesis and characterization of novel polyurethanes based on 4,4'-(1,4-phenylenebis[methylidene]nitro) diphenol. *Polym Bull* 60:609–616. <https://doi.org/10.1007/s00289-008-0896-8>
18. Wang W (2003) Synthesis and characterization of UV-curable polydimethylsiloxane epoxy acrylate. *Eur Polym J* 39:1117–1123. [https://doi.org/10.1016/S0014-3057\(02\)00374-9](https://doi.org/10.1016/S0014-3057(02)00374-9)
19. Ren X, Peng S, Zhang W, Yi C, Fang Y, Hui D (2017) Preparation of adipic acid-polyoxypropylene diamine copolymer and its application for toughening epoxy resins. *Compos B Eng* 119:32–40. <https://doi.org/10.1016/j.compositesb.2017.03.019>
20. Mishra JK, Kim I, Ha CS (2003) New millable polyurethane/organoclay nanocomposite: preparation, characterization and properties. *Macromol Rapid Commun* 24:671–675. <https://doi.org/10.1002/marc.200350008>
21. Madakbaş S, Türk Z, Şen F, Kahraman MV (2017) Thermal and morphological properties of organo modified nanoclay/polyethylene terephthalate composites. *J Inorg Organomet Polym* 27:31–36. <https://doi.org/10.1007/s10904-016-0438-z>
22. El-Fattah MA, El Saeed AM, Dardir MM, El-Sockary MA (2015) Studying the effect of organo-modified nanoclay loading on the thermal stability, flame retardant, anti-corrosive and mechanical properties of polyurethane nanocomposite for surface coating. *Prog Org Coat* 89:212–219. <https://doi.org/10.1016/j.porgcoat.2015.09.010>
23. Mallakpour S, Dinari M (2012) Synthesis and properties of biodegradable poly(vinyl alcohol)/organoclay bionanocomposites. *J Polym Environ* 20:732–740. <https://doi.org/10.1007/s10924-012-0432-7>

**Publisher's Note** Springer Nature remains neutral with regard to jurisdictional claims in published maps and institutional affiliations.

Springer Nature or its licensor holds exclusive rights to this article under a publishing agreement with the author(s) or other rightsholder(s); author self-archiving of the accepted manuscript version of this article is solely governed by the terms of such publishing agreement and applicable law.